

Original Research

The Prognostic and Immune Significance of BZW2 in Pan-Cancer and its Relationship with Proliferation and Apoptosis of Cervical Cancer

Chaolin Li^{1,†}, Qin Li^{1,†}, Li Li¹, Siyu Sun¹, Xun Lei^{1,*}¹Jinniu Maternity and Child Health Hospital of Chengdu, 610000 Chengdu, Sichuan, China*Correspondence: JNFY_leixun@163.com (Xun Lei)

†These authors contributed equally.

Academic Editor: Taeg Kyu Kwon

Submitted: 20 October 2023 Revised: 12 December 2023 Accepted: 27 December 2023 Published: 11 March 2024

Abstract

Background: Basic leucine zipper and W2 domains 2 (*BZW2*), a member of the basic domain leucine zipper superfamily of transcription factors, has been implicated in the development and progression of various cancers. However, the precise biological role of *BZW2* in pan-cancer datasets remains to be explored. This study aimed to assess the prognostic significance of *BZW2* and its immune-related signatures in various tumors. **Methods:** Our study investigated the expression, epigenetic modifications, and clinical prognostic relevance of *BZW2* using multi-omics data in different cancer types. Additionally, the immunological characteristics, tumor stemness, drug sensitivity, and correlation of *BZW2* with immunotherapy response were explored. Finally, *in vitro* experiments were conducted to assess the impact of *BZW2* knockdown on HeLa cells, a cell line derived from cervical squamous cell carcinoma and endocervical adenocarcinoma (CESC). **Results:** *BZW2* exhibited elevated expression levels in various tumor tissues and significantly impacted the prognosis of different cancer types. *BZW2* emerged as an independent prognostic factor in CESC. We found that copy number amplification and methylation levels of *BZW2* were associated with its mRNA expression. Immunological analyses revealed that *BZW2* shapes a non-inflamed immunosuppressive tumor microenvironment across multiple cancers. Furthermore, our cell experiments demonstrated that *BZW2* knockdown reduced proliferation, migration, and apoptosis activities in CESC cells. **Conclusions:** *BZW2* promotes cancer progression by shaping a non-inflamed immunosuppressive tumor microenvironment. Additionally, *BZW2* was shown to significantly influence the proliferation, migration, and apoptosis of CESC cells.

Keywords: BZW2; CESC; immunity therapy; apoptosis; biomarkers

1. Introduction

Cancer remains a substantial global health challenge, imposing significant burdens on public health systems worldwide [1]. According to projections made by the American Cancer Society, there will be around 1.91 million new instances of cancer in the US in 2022, with 600,000 cancer-related deaths expected as a result [2]. The impact of cancer is particularly pronounced in China, with an estimated 4.82 million new cancer cases and 3.21 million cancer-related deaths in the same year [3]. Consequently, cancer has become an urgent issue, requiring immediate attention. The advent of immunotherapy has instilled hope in patients with cancer, with notable advancements in the development of immune checkpoint inhibitors and chimeric antigen receptor (CAR) T-cell therapies [4,5]. These treatments have demonstrated significant effectiveness in the management of various malignant tumors, including melanoma [6], non-small cell lung cancer [7], and non-Hodgkin lymphoma [8]. However, the limited applicability of immunotherapy due to its specificity poses a significant challenge [9]. Consequently, there is an imminent need to uncover the specific immunological signatures associated with different cancer types and identify new targets that can be effectively utilized in immunotherapy. More-

over, there is an urgent requirement to actively seek alternative therapeutic targets and novel tumor biomarkers to enhance cancer diagnosis and treatment.

Basic leucine zipper and W2 domains 2 (*BZW2*) belongs to the basic leucine zipper (bZIP) superfamily of transcription factors [10]. Initially considered a novel protein interacting with E-cadherin, *BZW2* has been associated with multiple processes in cancer [11]. Wu *et al.* [12] were the first to employ a combined analysis of mouse and human microarray data, along with chromatin immunoprecipitation, to identify genes closely associated with c-MYC-induced tumors. Their findings indicated the involvement of *BZW2* in tumorigenesis. Jin *et al.* [13] further demonstrated that *BZW2* promotes the progression of hepatocellular carcinoma (HCC) by modulating the PI3K/AKT/mTOR signaling pathway. Li *et al.* [14] clarified the process by which *BZW2* mediates c-Myc expression, acting as an oncogene in the development of HCC. A recent study also showed that high *BZW2* expression affects the immune response of pancreatic adenocarcinoma (PAAD) and is an independent predictor of poor prognosis of PAAD [15]. These results imply that *BZW2* may be a useful predictive biomarker and a possible target for treatment. However, despite our current understanding of the mechanisms



and functions of *BZW2* in certain cancers, a comprehensive evaluation of its prognosis, epigenetic changes, and immunological characteristics across diverse cancer types is lacking. Therefore, in this study, we comprehensively analyzed *BZW2* expression and prognostic epigenetic changes across various cancer types. Additionally, we evaluated the immunological characteristics of *BZW2* in pan-cancer and its correlation with immunotherapy response and performed cell experiments to verify its potential role in cervical squamous cell carcinoma and endocervical adenocarcinoma (CESC). Our study aims to enhance our understanding of *BZW2* immune signatures in tumors and provide new insights into immunotherapy.

2. Materials and Method

2.1 Datasets Acquisition

The Gene Expression Omnibus (GEO) database was used to retrieve four cancer-related datasets, including GSE9750 for cervical cancer, GSE19804 for lung cancer, GSE17025 for endometrial cancer, and GSE43837 for breast cancer.

The University of California Santa Cruz (UCSC) Xena website (<https://xenabrowser.net/datapages/>) provided the mRNA normalized expression profiles, phenotype data, normal tissues in the Genotype-Tissue Expression (GTEx) database, DNA methylation profiles, and copy number variations (CNV) data for 33 different cancer types. The Cancer Cell Line Encyclopedia (CCLE, <https://sites.broadinstitute.org/ccle/>) was used to download data on cell line expression. Genomic Data Commons (GDC) (<https://portal.gdc.cancer.gov/>) provided the level 4 simple nucleotide variation (SNV) dataset for all The Cancer Genome Atlas (TCGA) samples processed using MuTect2 software (version 4.1.0.0, illumine, Inc., San Diego, CA, USA) [16]. The mRNA expression profiles of immune cells were obtained from both the Human Protein Atlas (HPA) database (<https://www.proteinatlas.org/>) and the study by Monaco *et al.* [17]. Data on microsatellite instability (MSI) and tumor mutation burden (TMB) for 33 different cancer types were gathered from research by Thorsson *et al.* [18] and Bonnevillie *et al.* [19], respectively. Data on the infiltration of pan-cancer immune cells were gathered from the Tumor Immune Estimation Resource 2.0 (TIMER2.0, <http://timer.cistrome.org/>). The Tracking Tumor Immunophenotype meta-server (<http://biocc.hrbmu.edu.cn/TIP/index.jsp>) was used to download immune activity ratings. The source of The Cancer Immunome Atlas (TCIA, <https://tcia.at/home>) provided the immunophenscore (IPS). Furthermore, for association analysis with *BZW2* expression, each tumor's epigenetically regulated RNA expression-based (EREG.EXPss) and RNA expression-based (RNAss) tumor stemness scores were used from earlier work [20].

2.2 Analysis of Immune Signatures, Stemness Scores, and Drug Sensitivity of *BZW2* in Pan-Cancer

Our study utilized the method developed by Zeng *et al.* [21] to examine the correlation between *BZW2* and the tumor microenvironment in a cohort of 33 tumors. The StromalScore, ImmuneScore, and ESTIMATEscore of tumor samples were computed using the R program ESTIMATE, and their connection with *BZW2* was evaluated [22]. *BZW2* and immune cell infiltration were compared in several cancer types using single sample gene set enrichment analysis (ssGSEA) and xCell methods [23,24]. The Tumor Immune Dysfunction and Exclusion (TIDE) algorithm and IPS from the TCIA database were utilized to evaluate the immunotherapy response. To compute the stemness index and evaluate its relationship with *BZW2* expression, Malta *et al.*'s [20] one-class logistic regression machine learning algorithm (OCLR) was employed. Based on the "oncoPredict" package, the relationship between *BZW2* and the IC50 of medicines from the Genomics Database of Cancer Drug Sensitivity V2 (GDSC V2, <https://www.cancerrxgene.org/>) was assessed [25,26].

2.3 Gene Set Variation Analysis (GSVA) and Correlation Analysis

Using transcriptome data from TCGA, GSVA enrichment analysis was carried out to assess the biological role of *BZW2* in cancers. 50 pathway gene sets were analyzed for enrichment in each pan-cancer sample based on the HALLMARK pathway set from the Molecular Signatures Database (<https://www.gsea-msigdb.org/gsea/index.jsp>). The Spearman correlation between *BZW2* and each HALLMARK pathway is then determined. Furthermore, pathways associated with immune inflammation were retrieved from the Kyoto Encyclopedia of Genes and Genomes (KEGG) official website (<https://www.kegg.jp/>). Immune-inflammation-related pathway scores were calculated using the ssGSEA method, and their relationship to *BZW2* was evaluated.

2.4 Clinical Prognostic Value of *BZW2* in Pan-Cancer

To assess the clinical prediction value of *BZW2*, survival data for pan-cancer, such as overall survival (OS), progression-free interval (PFI), disease-free interval (DFI), and disease-specific survival (DSS), were obtained from the TCGA database. The *BZW2* high expression and low expression groups comprised all patients of each cancer type, according to the best cutoff value. To examine the relationship between *BZW2* expression and patient prognosis, Cox analysis and Kaplan-Meier (KM) survival curves were produced using the R packages "survival" and "survminer" and then analyzed. To examine the prediction accuracy of the *BZW2*, TimeROC (receiver operating characteristic) study was used. In order to find independent predictive indicators, univariable and multivariable Cox regression analyses were undertaken.

2.5 Cell Culture, RNA Extraction, and Quantitative Real-Time PCR (qRT-PCR)

Hela cells were obtained from the Chinese Academy of Sciences' Cell Bank in Shanghai, China. The cells were grown in DMEM medium (HyClone, Inc., Logan, UT, USA) containing 10% fetal bovine serum (Vazyme biotech co., Nanjing, Jiangsu, China), 100 mg/mL streptomycin and 100 U/mL penicillin. Cells were incubated in a humidified atmosphere with 5% CO₂ at 37 °C. Total RNA was isolated using the TRIzol reagent (Invitrogen, Inc., Carlsbad, CA, USA), as directed by the manufacturer. 1 µg of RNA was used for cDNA synthesis by the Hiscript III 1st strand cDNA synthesis kit (Vazyme biotech co., Nanjing, China). *GAPDH* was amplified from each sample to ensure equal cDNA input. Each PCR reaction contained 1 µL of cDNA, 0.6 µL of forward and reverse primers (10 µM), 7.5 µL of ChamQ Universal SYBR qPCR Master Mix (Vazyme biotech co., Nanjing, China), and 6.3 µL of ddH₂O. The PCR reaction parameters were as follows: 10 minutes of pre-denaturation at 95 °C, 40 cycles of denaturation for 15 seconds at 95 °C, 1 minute of annealing at 62 °C, and 15 seconds of extension at 72 °C. A reaction was required at 60 °C for one minute and 95 °C for fifteen seconds in the last extension phase. The forward and reverse primers for *GAPDH* were GGAGCGA-GATCCCTCCAAAAT and GGCTGTTGTCATACTTCT-CATGG, respectively. The forward and reverse primers for *BZW2* were CCAGTCTCTTCACCGACAGCTT and GACGAGGTAACAGAGTTGGCATC, respectively. The Hela cells line were validated by short tandem repeat profiling and tested negative for mycoplasma.

2.6 Western Blotting

Cells were harvested following treatment with siRNAs. The cells were then collected by centrifugation after being cleaned three times with phosphate-buffered saline (PBS). Proteinase inhibitors (#R0010, Solarbio, Inc., Beijing, China) were added to RIPA buffer to help create total protein extracts. *BZW2* (#ab254772, Abcam, Inc., Shanghai, China) and *GAPDH* (#60004-1-Ig, Proteintech Group, Inc., Wuhan, China) antibodies were used in line with the manufacturer's instructions for western blot analysis. Goat Anti-Mouse IgG-HRP (#SA00001-1, Proteintech Group, Inc., Wuhan, China) and Goat Anti-Rabbit IgG-HRP (#SA00001-2, Proteintech Group, Inc., Wuhan, China) were the secondary antibodies used. The protein loading control was GAPDH. The enhanced chemiluminescence (ECL) reagent (Beijing 4A Biotech Co., Ltd., Beijing, China) was used to visualize the signals.

2.7 Counting Kit-8 (CCK8) Detection and Transwell Migration Assay

Hela cells transfected with siRNAs-*BZW2* were harvested upon reaching 90% confluency. They were then seeded onto 96-well culture plates, with five multiple wells

allocated to each group, and 5000 cells per well. The CCK-8 kit (#KGA9310-1000, Nanjing KeyGen Biotech. Inc., Nanjing, China) was used to examine the cells at 0 h, 24 h, 48 h, and 72 h after they were incubated in an incubator with 37 °C and 5% CO₂.

The 24-well Transwell chamber (Corning, Inc., Corning, NY, USA) was set up and left at 4 °C for the whole night. Transwell insert was then seeded with a 200 µL cell solution comprising 100,000 cells/mL. The lower chamber was then filled with a culture medium (700 µL) containing 10% Fetal Bovine Serum (FBS). After 24 h of culture, cell fixation was performed using 4% paraformaldehyde at room temperature for 20 minutes, followed by staining with 0.5% crystal violet dye for 5 minutes. The cell count was recorded thereafter.

2.8 Flow Cytometric Analysis of Apoptosis

After being harvested, Hela cells were suspended in a binding buffer. The cells were then stained in accordance with the manufacturer's instructions using the Annexin V-APC/PI Apoptosis Detection Kit (Nanjing KeyGen Biotech. Inc., Nanjing, China). A Beckman Cytoflex device was used for the flow cytometry analysis, and CytExpert Software (version 2.0, Beckman Coulter, Inc., Brea, CA, USA) was used to analyze the data.

2.9 Statistical Analysis

R software (version 4.0.3; <https://www.r-project.org/>) was used for all analysis techniques with the exception of internet tools. Tumor and normal sample differential expression was computed using the Wilcoxon rank-sum test. The Spearman and Pearson correlation approach was used to conduct correlation analysis. For the analysis of cell experiment data, GraphPad Prism for Windows (version 9.0.0, GraphPad Software, Inc., San Diego, CA, USA) was used. Three biological replicates of each experiment were conducted and the standard deviation is used to characterize the degree to which the data deviates from the mean. The Student's *t*-test was used to determine statistical significance, with *p*-values of less than 0.05 being regarded as significant. The following were used to indicate the significance levels: **p* < 0.05, ***p* < 0.01, ****p* < 0.001.

3. Results

3.1 *BZW2* is Upregulated in Multiple Cancer Types in Pan-Cancer

We initially examined the expression of *BZW2* in human normal tissues and observed higher levels of *BZW2* expression in tissues such as bone marrow, muscle, and heart (**Supplementary Fig. 1A**). High expression of *BZW2* was found in cancer cell lines including stomach adenocarcinoma (STAD) and skin cutaneous melanoma (SKCM) after analysis of the expression patterns of tumor cell lines (**Supplementary Fig. 1B**). The TCGA data further confirmed elevated levels of *BZW2* in tumor tissues

such as rectum adenocarcinoma (READ), colon adenocarcinoma (COAD), and esophageal carcinoma (ESCA) (Supplementary Fig. 1C). Additionally, we observed higher expression of *BZW2* in myeloid dendritic cells (Supplementary Fig. 1D,E). Upon merging GTEx and TCGA samples, we observed significant upregulation of *BZW2* expression in over 70% of tumor types, including breast invasive carcinoma (BRCA), CESC, lymphoid neoplasm diffuse large B-cell lymphoma (DLBC), brain lower grade glioma (LGG), and thymoma (THYM) (Fig. 1A). *BZW2* was significantly upregulated in a number of tumor tissues when compared to paired normal neighboring tissues in the TCGA pan-cancer dataset (Supplementary Fig. 2A–P). We also studied *BZW2* expression in four GEO datasets, which revealed that *BZW2* expression was significantly higher in cervical cancer (Fig. 1B), lung cancer (Fig. 1C), and endometrial cancer (Fig. 1D) compared with normal tissues. Additionally, we observed high *BZW2* expression in metastatic breast cancer (Fig. 1E). *BZW2* was substantially increased at the protein expression level in ten different cancer types according to the Clinical Proteomic Tumor Analysis Consortium database. These cancers include breast cancer, colon cancer, ovarian serous cystadenocarcinoma (OV), clear cell renal cell carcinoma (ccRCC), uterine corpus endometrial carcinoma (UCEC), lung cancer, PAAD, head and neck squamous cell carcinoma (HNSC), glioblastoma multiforme (GBM) and liver cancer (Fig. 1F). Additional immunohistochemistry investigation confirmed that *BZW2* is highly expressed on the protein level in a variety of malignancies (Supplementary Fig. 3). These results indicate that *BZW2* is upregulated in multiple cancer types, suggesting its potential role in cancer initiation and progression.

3.2 *BZW2* is Regulated by Copy Number Amplification and DNA Methylation

We examined *BZW2*'s SNV and CNV as well as alterations in DNA methylation in the *BZW2* promoter region to identify the mechanism causing elevated *BZW2* expression. The SNV of *BZW2* were primarily missense mutations, with UCEC ($n = 175$, 3.4%) exhibiting the highest SNV rate (Supplementary Fig. 4A). Furthermore, we observed a higher frequency of copy number amplifications of varying degrees in most cancer types as compared to copy number deletions (Fig. 2A). Multiple cancer types also showed a substantial positive connection between *BZW2* mRNA expression and CNV (Supplementary Fig. 4B). The four most relevant cancer types were ESCA ($r = 0.568$, Supplementary Fig. 4C), HNSC ($r = 0.498$, Supplementary Fig. 4D), sarcoma (SARC) ($r = 0.517$, Supplementary Fig. 4E), and READ ($r = 0.514$, Supplementary Fig. 4F).

At the epigenetic level, we observed significant hypomethylation levels in tumor tissues in more probes (including cg23402769 in the promoter region and

cg25778479 in the *BZW2* body) than in normal tissues (Supplementary Fig. 5A). The results of correlation analysis showed that mRNA expression in the majority of tumor types, including BRCA, CESC, and lung squamous cell carcinoma (LUSC), was strongly negatively linked with the methylation levels of various locations in the *BZW2* promoter region and *BZW2* body (Fig. 2B). Notably, in cg25778479 and cg22294755 in one-third of cancer types, we found a substantial negative connection between *BZW2* mRNA expression and methylation levels (Supplementary Fig. 5B,C). TMB and MSI are key factors in clinical immunotherapy. Our analysis revealed a significant positive correlation between *BZW2* expression and TMB in COAD, THYM, lung adenocarcinoma (LUAD), STAD, pheochromocytoma and paraganglioma (PCPG), SARC, and prostate adenocarcinoma (PRAD) (Supplementary Fig. 5D). Additionally, Testicular germ cell tumors (TGCT), THYM, STAD, OV, and other cancers showed a significant positive correlation with MSI (Supplementary Fig. 5E). Moreover, we investigated the relationship between *BZW2* mRNA expression and *TP53* mutations and discovered a consistent positive link in a variety of malignancies, including BRCA, COAD, HNSC, liver hepatocellular carcinoma (LIHC), LUAD, PAAD, PRAD, and UCEC (Supplementary Fig. 5F). These findings together shed light on the regulatory mechanisms by which *BZW2*'s DNA copy number amplification and DNA demethylation encourage the upregulation of its mRNA in different cancer types, which may be essential for the development and spread of cancer.

3.3 *BZW2* Shapes Non-Inflamed Tumor Microenvironment in Multiple Cancer Types

Conducting a comprehensive pan-cancer analysis to elucidate the immunological effects of *BZW2* is vital for identifying cancer types that might benefit from anti-*BZW2* immunotherapy. The expression of *BZW2* mRNA was shown to be highly correlated with immunological subtypes in various forms of cancer. Specifically, *BZW2* exhibited enhanced expression in the C1 subtype (associated with wound healing) of most cancers, including bladder urothelial carcinoma (BLCA), COAD, and LIHC, while it showed lower expression in C3 (associated with inflammation) (Supplementary Fig. 6). Furthermore, *BZW2* showed noteworthy negative relationships with the ImmuneScore, EstimateScore, and StromalScore in a variety of cancer types, such as CESC and STAD (Fig. 3A). Besides, we observed significant positive correlations between *BZW2* and mismatch-related signatures across almost all cancer types, while significant negative correlations were observed with immune-related signatures in most cancers (Supplementary Fig. 7A). These results point to a possible involvement of *BZW2* in the development of different types of cancers.

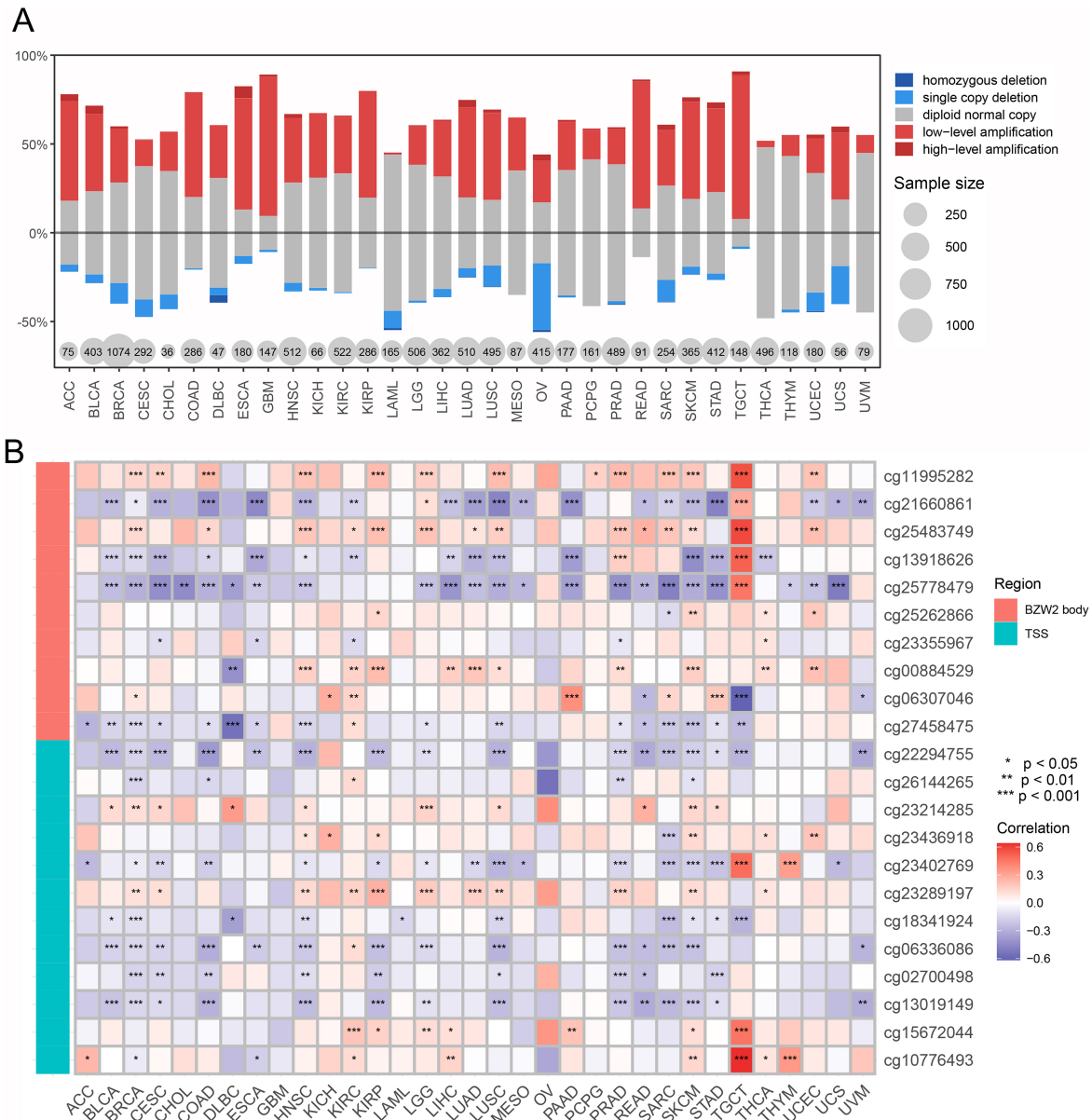


Fig. 2. 33 cancer types were subjected to examination of (A) DNA copy number variation and (B) DNA methylation.

chemokines, and immune stimulators, and assessed their relationships with *BZW2*. We found a negative correlation of *BZW2* with most immunomodulators in pan-cancer, and this negative correlation was particularly pronounced in MHC (**Supplementary Fig. 8**). These findings indicate that high *BZW2* expression may downregulate antigen presentation and processing capabilities. Moreover, several chemokine receptors were also observed to be significantly negatively correlated with *BZW2*, including *CXCR3*, which mediates the chemotaxis and activation of T lymphocytes and natural killer cells, and *CXCR5*, which regulates the chemotaxis and activation of B cells. However, the multifaceted functions of the chemokine system warrant further investigation, and these results alone are insufficient to elucidate the overall immune role of *BZW2* in the tumor microenvironment.

Chemokines and their receptors are immune regulatory elements whose actions are directly reflected in the activity of the cancer immune cycle. Our analysis reveals a significant negative correlation between *BZW2* and various steps of the cancer immune cycle, including antigen release (Step 1) and priming and activation (Step 3), in cancers, including BRCA, COAD, ESCA and other cancers (**Supplementary Fig. 9**). Additionally, trafficking of immune cells to tumors, such as CD8⁺ T cell recruiting, Macrophage recruiting, Th1 cell recruiting, NK cell recruiting, and Dendritic cell recruiting (Step 4), is also significantly negatively correlated with *BZW2* in several cancer types, including BRCA, SKCM, TGCT, and THCA. Reduced activity of these steps may reduce the infiltration of effector tumor-infiltrating immune cells in the tumor microenvironment. Notably, a significant negative correla-

tion was observed between the infiltration of immune cells into tumors (Step 5) and *BZW2* in more than 20 cancer types (**Supplementary Fig. 9**). These findings underscore *BZW2*'s role in shaping a non-inflamed immunosuppressive tumor microenvironment in various cancers.

Considering the immunosuppressive role of *BZW2* in tumors, we evaluated its responsiveness to predict immune checkpoint blockade (ICB) treatment. Higher TIDE scores indicate worse ICB efficacy and shorter post-treatment survival. Notably, in GBM, kidney renal clear cell carcinoma (KIRC), LGG, LIHC, LUAD, PCPG, READ, SARC, and TGCT, we found higher TIDE scores in the *BZW2* high-expression group. This suggests that the *BZW2* low-expression group has superior ICB efficacy and longer post-treatment survival (**Supplementary Fig. 10A–I, Supplementary Table 2**). What's more, we employed the IPS to assess the response to immunotherapy. Stronger immunogenicity and better immunotherapy benefit are correlated with higher IPS values. Our findings demonstrated that the *BZW2* low-expression group of GBM, KIRC, and LUAD patients exhibited stronger immunogenicity when treated with *PDI*, *CTLA4*, and combination therapy (**Supplementary Fig. 10J–L**).

3.4 *BZW2* is Associated with Tumor Stemness and Drug Sensitivity

Cancer stem cells have the potential to self-renew and differentiate in several directions, and they may continually make new tumor cells, which is critical for tumor formation and progression. We evaluated the correlation between *BZW2* expression and two tumor stemness indices (EREG.EXPss and RNAss). The stemness score and *BZW2* expression in various malignancies showed a strong positive connection, according to our data (Fig. 4A–C). Additionally, we also evaluated the stemness index of pan-cancer samples using the OCLR algorithm and found that the *BZW2* high expression group exhibited higher stemness scores in multiple cancers (Fig. 4D). These findings suggested that elevated *BZW2* expression may promote the stemness characteristics of cancer cells, thus affecting autophagy activity.

We also assessed the correlation between the *BZW2* gene and 198 drugs, revealing significant negative correlations between *BZW2* and 28 drugs, such as Gefitinib and Afatinib. Subsequent analysis indicated that these drugs with significant correlations predominantly targeted the EGFR pathway (**Supplementary Fig. 11**), highlighting the potential significance of the *BZW2* gene in regulating this pathway.

3.5 *BZW2* is Associated with Multiple Cancer-Related Pathways

We performed a GSVA enrichment analysis to gather knowledge about the possible roles and processes of *BZW2* in pan-cancer. A number of cancer-related pathways, such

as MYC targets (Fig. 5B), G2/M checkpoint, mTORC1 signaling (Fig. 5C), E2F targets, PI3K AKT mTOR signaling, and DNA repair, were considerably enriched, as Fig. 5A illustrates. Additionally, we also observed a significant negative correlation between *BZW2* and KRAS signaling dn (Fig. 5D) and inflammatory response pathways (Fig. 5E) in some cancers. Furthermore, we found that *BZW2* and immune-inflammatory pathways significantly correlated negatively in more than half of the cancer types (Fig. 5F). Correlation analysis also uncovered a significantly positive correlation between *BZW2* expression and multiple oncogenes (Fig. 5G).

3.6 *BZW2* is an Independent Prognostic Factor in CESC

The expression of *BZW2* mRNA is strongly linked to a poor prognosis in a variety of cancer types. In particular, worse OS, DSS, and PFI were substantially correlated with higher *BZW2* expression in adrenocortical carcinoma (ACC), CESC, LIHC, LUAD, PAAD, and SARC. Furthermore, poorer OS in HNSC and thyroid cancer (THCA), worse DSS in kidney chromophobe cell carcinoma (KICH), KIRC, and PRAD, and worse PFI in HNSC, KICH, and KIRC were all significantly correlated with increased *BZW2* expression (Fig. 6A, **Supplementary Fig. 12A**). *BZW2* has been discovered as a prognostic factor for a variety of malignancies, including CESC (Fig. 6A–E). Diagnostic ROC curve analysis revealed that the area under the curve (AUC) for CESC was 0.956, with the AUC of *BZW2* effectively predicting the overall recurrence rate at 1, 2, and 3 years (0.712, 0.646, and 0.666, respectively) (Fig. 6F,G). *BZW2* was found to be an independent predictive factor for CESC in univariate and multivariate Cox regression models (Fig. 6H).

We looked at the relationship between *BZW2* and CESC clinical characteristics since there is a strong link between *BZW2* and the clinical prognosis of CESC. Our findings revealed significant correlations between *BZW2* and both age and grade stage in CESC (**Supplementary Fig. 12B–D**). Notably, as the malignancy of CESC increased, there was a gradual increase in the expression level of *BZW2*, indicating its close association with CESC development.

3.7 *BZW2* Regulates Cervical Cancer Cell Proliferation and Migration

Expression levels of *BZW2* in CESC cell lines were analyzed using CCLE data, revealing higher *BZW2* expression in HeLa cells (Fig. 7A). HeLa cells were therefore chosen for further studies. HeLa cells were effectively transfected with two *BZW2* siRNA knockout vectors. The transfected group's effective suppression of mRNA and protein expression in comparison to the control group (siRNC) was shown by RT-PCR and western blot analysis (Fig. 7B,C). The cell viability post-transfection with siRNC, siRNA1, and siRNA2 was assessed using the CCK8 kit, revealing a

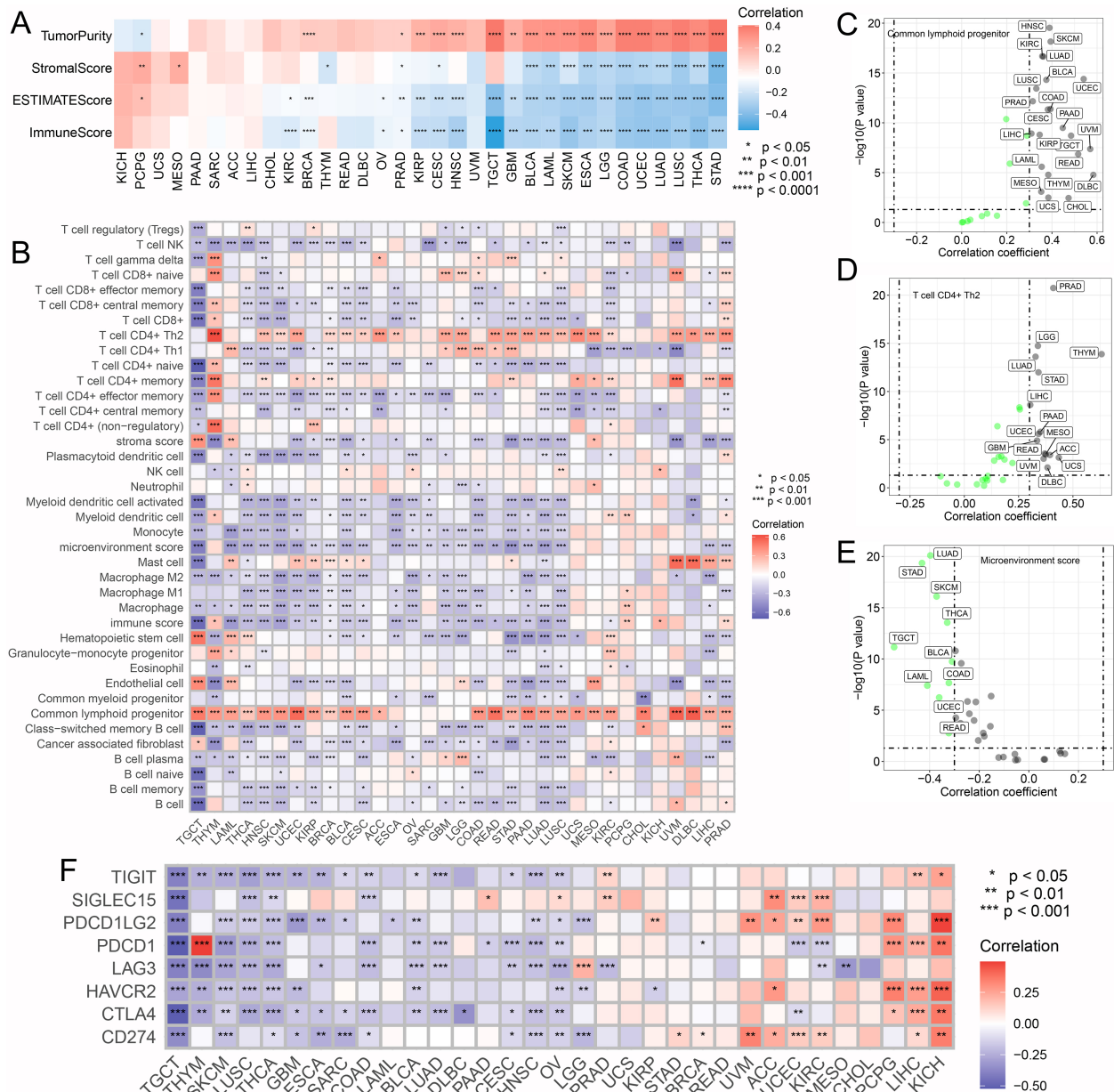


Fig. 3. Correlation of *BZW2* and immune signatures in pan-cancer. (A) The ESTIMATE algorithm evaluated the relationship between *BZW2* and tumor microenvironment. (B) The relationship between *BZW2* and immune cell infiltration is evaluated by the xCell algorithm. (C) The infiltration of common lymphoid progenitor cells was positively linked with *BZW2*. (D) The infiltration of T cell CD4⁺ Th2 cells was positively linked with *BZW2*. (E) *BZW2* was negatively correlated with microenvironment score. (F) Correlation between immune checkpoints and *BZW2* in pan-cancer.

significant reduction in cell proliferation ability after 24 h, 48 h, and 72 h of *BZW2* knockout (Fig. 7D). The cell apoptosis experiment further revealed that siRNC had an average apoptosis rate of 8.4%, but siRNA1 and siRNA2 had rates of 33.2% and 30.1%, respectively (Fig. 7E,F). Additionally, the Transwell experiment showed that *BZW2* deletion significantly reduced the capacity of Hela cells to migrate (Fig. 7G,H). All of these findings point to the critical function *BZW2* plays in controlling the migration and proliferation of cervical cancer cells.

4. Discussion

BZW2 is a well-established tumor-related gene with significant implications in the study of tumor biology [28]. It has been associated with various cancer types, such as osteosarcoma [29], colorectal cancer [30,31], lung adenocarcinoma [32] and fibrosarcoma [33]. Despite its acknowledged importance, a thorough investigation of all cancer types is currently required in order to evaluate *BZW2*'s differential expression, immunological markers, and epigenetic alterations in tumor heterogeneity. Here, we assessed

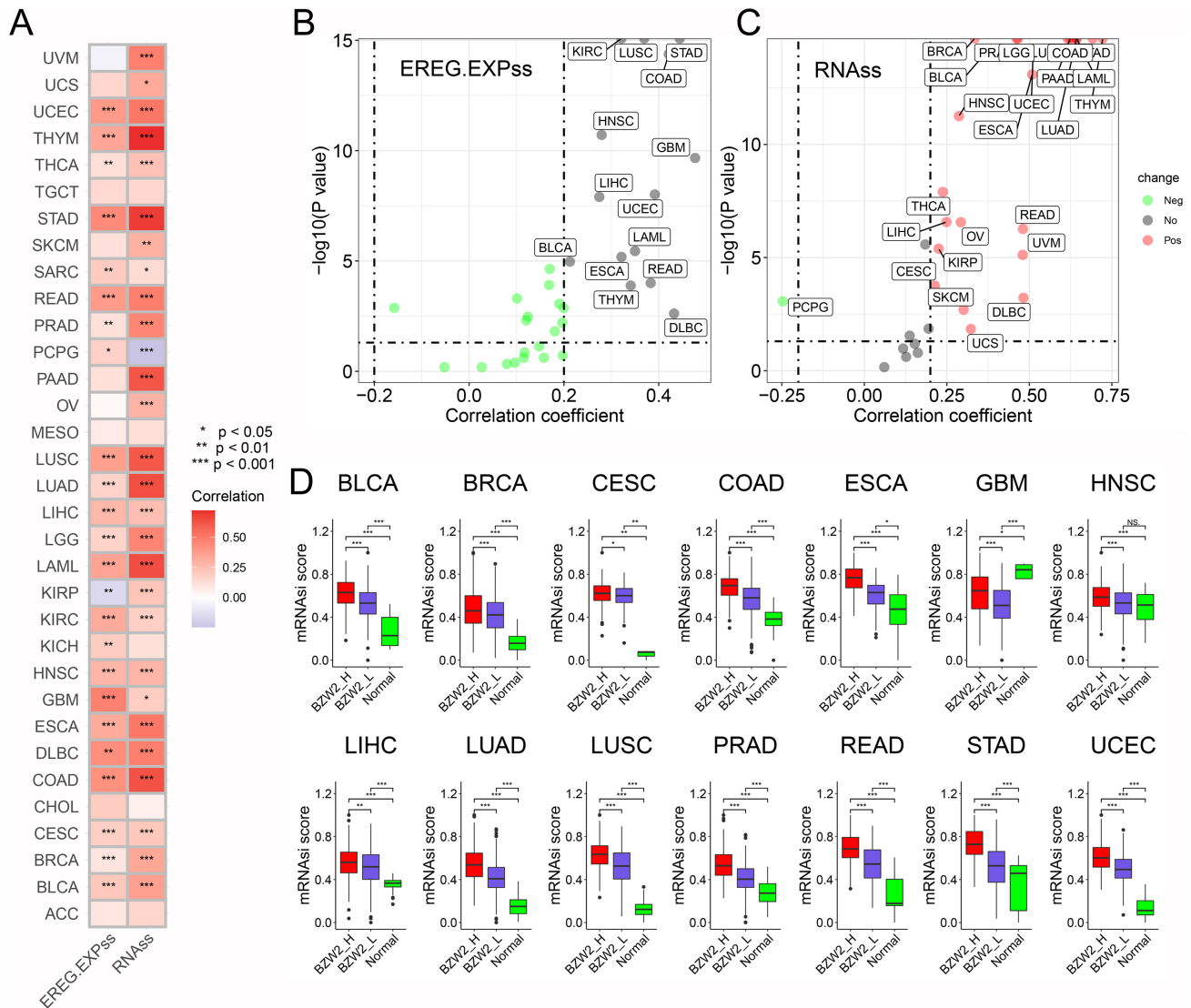


Fig. 4. Correlation between *BZW2* and cancer stemness. (A) *BZW2* was positively correlated with the stemness score of multiple cancers. (B) Relationship between *BZW2* and epigenetically regulated RNA expression-based (EREg.EXPss). (C) Relationship between *BZW2* and RNA expression-based (RNAss). (D) One-class logistic regression machine learning algorithm (OCLR) evaluates stemness score. * $p < 0.05$, ** $p < 0.01$, *** $p < 0.001$. EREG.EXPss, Epigenetically regulated RNA expression-based; RNAss, RNA stemness scores.

the differential expression of *BZW2* by the first pan-cancer investigation. Our findings demonstrate that *BZW2* expression is markedly elevated in the majority of malignancies, both in terms of mRNA and protein. The mRNA expression of *BZW2* is modulated by CNV and methylation levels. A previous study by Huang *et al.* [34] demonstrated that *METTL3* facilitates m6A methylation of *BZW2*, contributing to the progression of multiple myeloma. Our investigation, which made use of methylation data from the TCGA database, demonstrated the epigenetic changes of *BZW2* in a range of malignancies. Alterations in CNVs have the ability to influence signaling system activity and regulate the aberrant expression of many genes [35]. We found a significant negative correlation between *BZW2* mRNA expression

and its methylation level, while a significant positive correlation existed with CNV. Notably, this correlation appears to be cancer-type-dependent, emphasizing the role of epigenetic changes in mediating *BZW2* mRNA expression, which could be critical in the etiology and progression of cancer. The substantial copy number amplification of *BZW2* in most cancers could promote cancer progression. Importantly, these epigenetic modifications, involving aberrant methylation and CNVs of *BZW2*, are associated with poor prognosis in various cancers, highlighting their potential clinical impact on cancer outcomes. The *TP53* gene, a pivotal tumor suppressor gene, is closely linked to the onset and progression of various cancers [36]. Our analysis revealed a higher frequency of *TP53* mutations in the

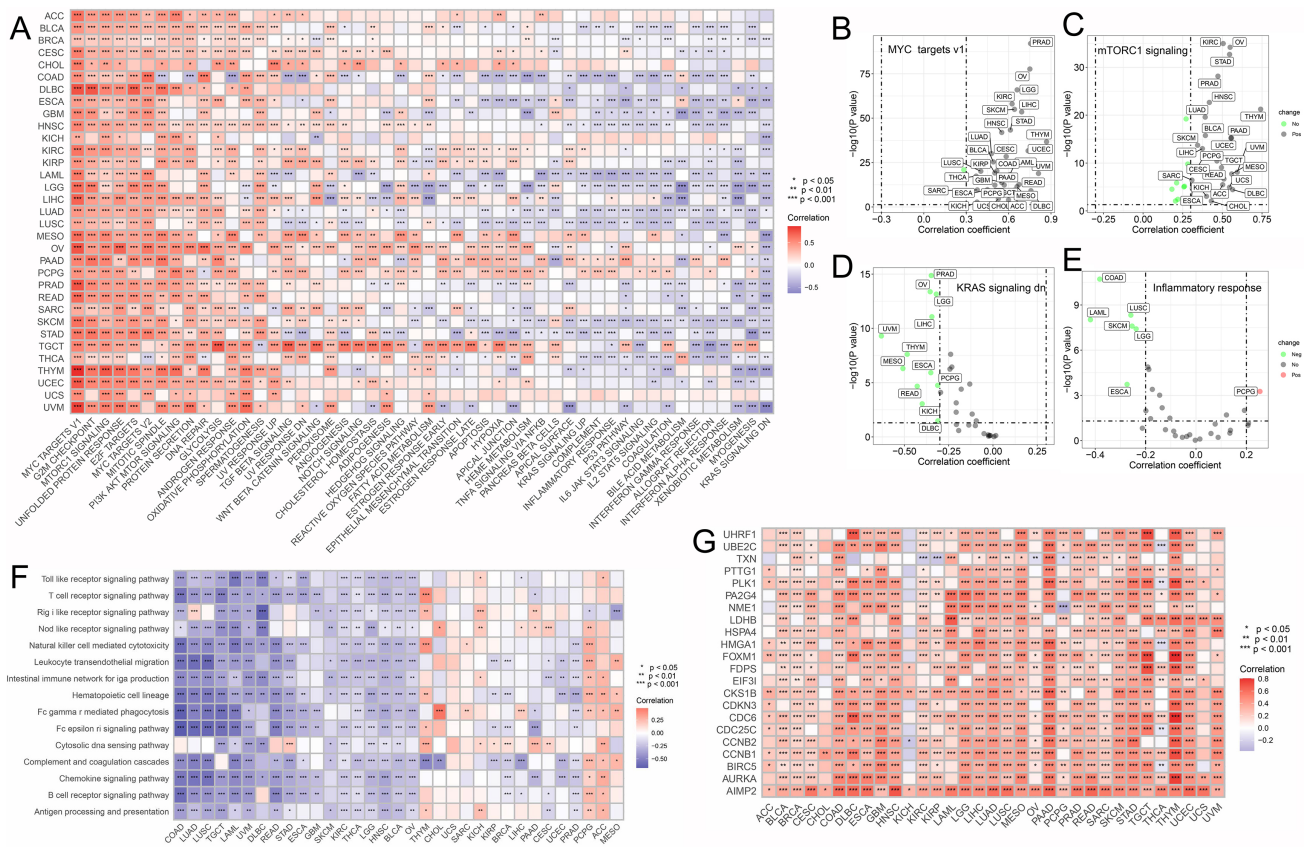


Fig. 5. Correlation between *BZW2* and cancer-related pathways. (A) Gene Set Variation Analysis (GSEA) enrichment analysis assesses the relevance of *BZW2* and pathways. (B) Correlation between MYC TARGETS V1 and *BZW2*. (C) Correlation between MTORC1 SIGNALING and *BZW2*. (D) Correlation between KRAS SIGNALING DN and *BZW2*. (E) Correlation between INFLAMMATORY RESPONSE and *BZW2*. (F) Correlation between *BZW2* and immune-inflammatory pathways. (G) Correlation between *BZW2* and oncogenes.

BZW2 high-expression group across multiple cancers. This result highlights the association between *BZW2* expression and *TP53* mutations, shedding light on how *TP53* gene mutations may influence tumor initiation and progression.

Dynamic changes in the tumor microenvironment and the degree of infiltration of different immune cells determine the progression of the tumor and the degree of response to immunotherapy [37]. The results of our study showed a substantial negative association with immune-associated aspects and a strong positive relationship between the *BZW2* gene expression and features related to mismatch repair. This suggests that *BZW2* may affect the mismatch repair mechanism, thus inhibiting tumor genome instability, but at the same time, it inhibits the immune system's response, leading to tumor escape and progression. The findings of the examination of immune cell infiltration further demonstrate *BZW2*'s immunosuppressive function in a variety of malignancies. Immunosuppressive properties of MDSC immune cells are well recognized [38]. They can lessen the immune system's capacity to combat cancer cells by suppressing the function of other immune cells. We found a considerable positive correlation between the infil-

tration of MDSC immune cells and the *BZW2* gene in many cancers. This implies that *BZW2* may increase the immunosuppressive effect by promoting the infiltration of immune cells known as MDSC, which in turn stimulates the growth of cancer. Additionally, we discovered a substantial negative correlation between *BZW2* and a number of immune regulatory factors as well as different stages of the cancer immune cycle. This finding implies that *BZW2* may depress the immune system by comprehensively downregulating the expression of many immunomodulators, which would lower the immune system's action against cancer. This leads to a decrease in the recruitment of effector immune cells and the promotion of a non-inflamed tumor microenvironment. Our results indicate that *BZW2* promotes cancer progression in multiple cancers by shaping a non-inflamed immunosuppressive microenvironment.

The stemness score is a valuable indicator, often associated with tumor malignancy and treatment response. A high stemness score indicates that tumor cells possess robust stemness characteristics, rendering them more resistant to chemotherapy and radiotherapy [39]. Our analysis has revealed that the *BZW2* low-expression group exhib-

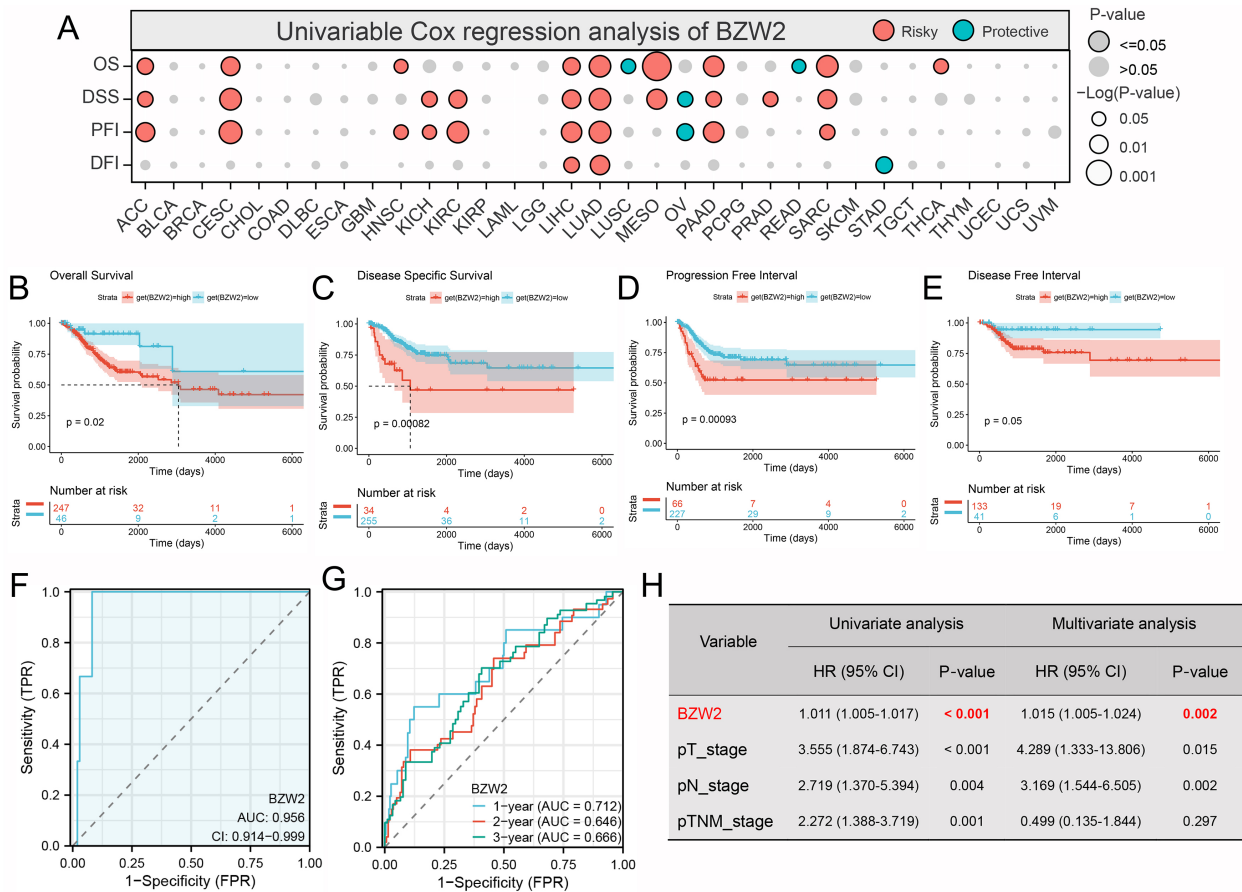


Fig. 6. Correlation between *BZW2* and pan-cancer prognosis. (A) Univariable cox regression analysis of *BZW2*. (B) Association between *BZW2* and overall survival in cervical cancer. (C) Association between *BZW2* and disease specific survival in cervical cancer. (D) Association between *BZW2* and progression free interval in cervical cancer. (E) Association between *BZW2* and disease free interval in cervical cancer. (F) Analysis of the diagnostic efficacy of *BZW2* in cervical cancer. (G) TimeROC (receiver operating characteristic) analysis of *BZW2* in cervical cancer. (H) Univariate and multivariate analysis results of *BZW2* in cervical squamous cell carcinoma and endocervical adenocarcinoma (CESC).

ited lower stemness scores across multiple cancers, suggesting that the *BZW2* gene plays a significant role in regulating the stemness characteristics of tumor cells. Further research is needed to uncover the mechanisms underlying tumor development and to develop new treatment strategies. Furthermore, our drug sensitivity analysis has identified a significant negative correlation between *BZW2* and multiple EGFR pathway-related drugs. This finding implies that tumor cells expressing high levels of the *BZW2* gene are less sensitive to drugs targeting the EGFR pathway. Therefore, the *BZW2* gene likely plays a role in the regulation of the EGFR pathway, affecting the responsiveness of tumor cells to related drugs. Also, a strong correlation between *BZW2* and various prognostic characteristics of CESC was found by survival analysis. *BZW2* was validated as an independent predictive factor for CESC in subsequent univariate and multivariate studies. These results demonstrate the significance of *BZW2* in carcinogenesis and prognosis as a whole. Furthermore, GSVA enrichment analysis demonstrated a substantial positive link between the *BZW2* gene

and the myc targets pathway, indicating that *BZW2* may have potential functions in cell proliferation, apoptosis, and cell cycle regulation. To verify this, we conducted cell experiments, which confirmed that *BZW2* knockdown significantly reduces proliferation, migration, and apoptosis of CESC Hela cell lines.

In conclusion, our research is the first thorough examination of the *BZW2* gene in a variety of cancer forms. Our work revealed that *BZW2* exhibits high expression in multiple tumor types and serves as an independent prognostic factor, particularly in CESC. Our study extensively examines the epigenetic modifications and immunological features of *BZW2* in pan-cancer. Moreover, experiments involving *BZW2* knockout demonstrate its impact on the proliferation, migration, and apoptosis of CESC cells. These findings shed light on the potential functional mechanisms and clinical prognostic characteristics of *BZW2* in pan-cancer and offer valuable insights for future immunotherapy research.

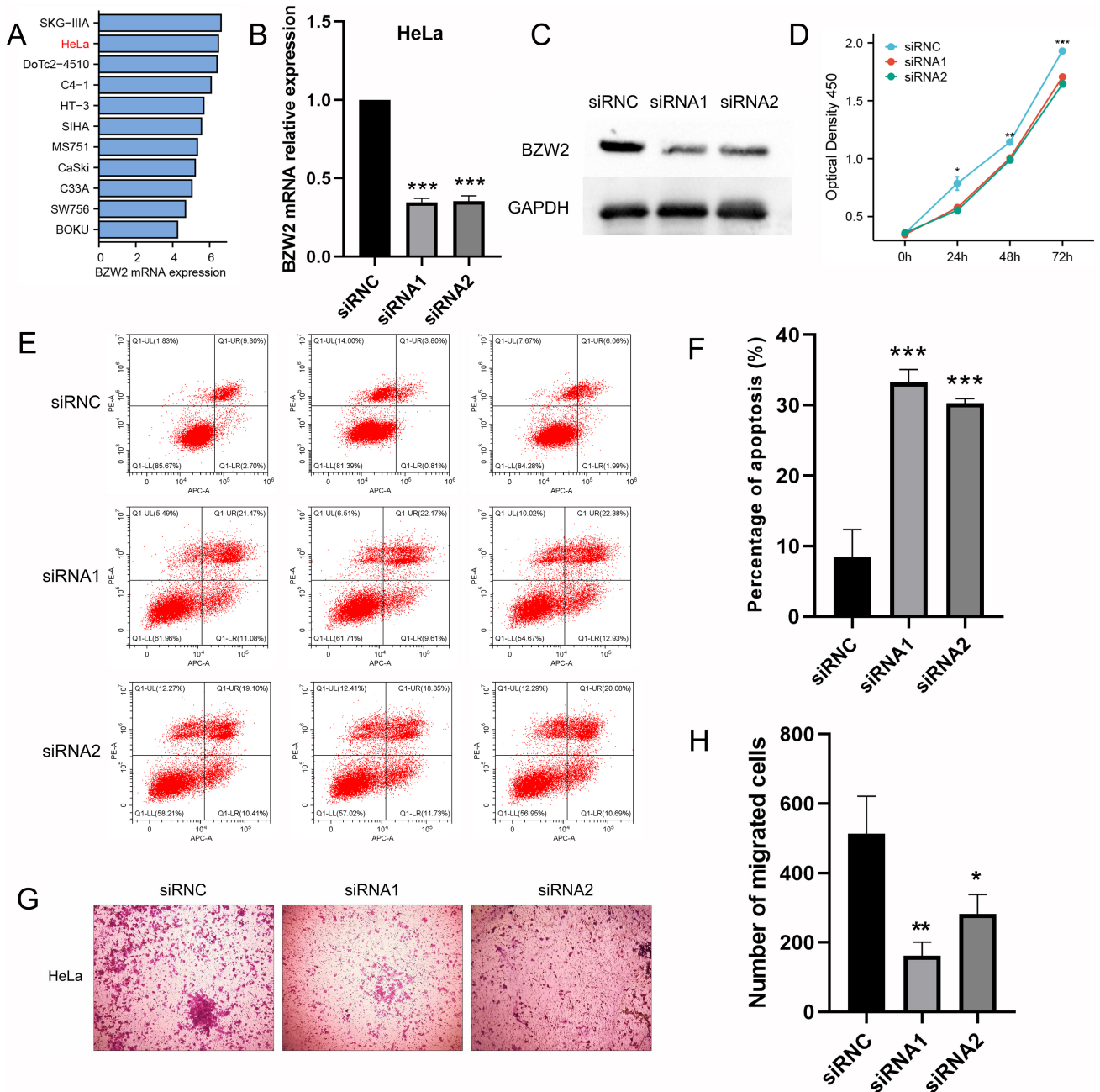


Fig. 7. *BZW2* knockdown's impact on the CESC cell line HeLa, a total of 3 biological replicates were performed for each set of experiments. (A) The Cancer Cell Line Encyclopedia (CCLE) dataset examined *BZW2* expression in several CESC cell lines. (B) Verification of *BZW2* knockdown effectiveness in HeLa cells using real-time polymerase chain reaction (RT-PCR). (C) By using Western blot, the knockdown effectiveness of *BZW2* in HeLa cells was confirmed. (D) Using the Cell Counting Kit-8 (CCK8) test, examine how *BZW2* knocked affects cell proliferation. (E) The rate of apoptosis in HeLa cells with cervical cancer was increased by *BZW2* knocked. (F) The percentage of apoptotic cells in the three groups. (G) *BZW2* deletion significantly reduced the capacity of HeLa cells to migrate. (H) The number of migrated cells in the three groups. * $p < 0.05$, ** $p < 0.01$, *** $p < 0.001$. The Transwell experiment results are generated under a 40 \times magnification, and the scale bar is 100 μm .

5. Conclusions

In summary, based on a global pan-cancer perspective, we found that *BZW2* promotes cancer progression by forming a non-inflammatory immunosuppressive tumor microenvironment. In addition, *BZW2* can also signifi-

cantly affect the proliferation, migration and apoptosis of CESC cells. Our findings may help understand the association between *BZW2* and cancer progression and provide ideas for immunotherapy research.

Availability of Data and Materials

The data that support the findings of this study are available from the corresponding author on reasonable request.

Author Contributions

All authors contributed to the study conception and design. Material preparation, data collection and analysis were performed by CL, QL, LL, SS and XL. QL and CL jointly completed the cell experiments. The first draft of the manuscript was written by CL and all authors commented on previous versions of the manuscript. All authors contributed to editorial changes in the manuscript. All authors read and approved the final manuscript. All authors have participated sufficiently in the work and agreed to be accountable for all aspects of the work.

Ethics Approval and Consent to Participate

Not applicable.

Acknowledgment

We thank Bullet Edits Limited for the linguistic editing and proofreading of the manuscript.

Funding

This study was funded by scientific research project of Sichuan Maternal and Child Health Association (No. 22FXZD04) and general Project of Scientific Research Project of Jinniu District Medical Association, Chengdu City, Sichuan Province (JNKY2021-52).

Conflict of Interest

The authors declare no conflict of interest.

Supplementary Material

Supplementary material associated with this article can be found, in the online version, at <https://doi.org/10.31083/j.fbl2903097>.

References

- [1] Leiter A, Veluswamy RR, Wisnivesky JP. The global burden of lung cancer: current status and future trends. *Nature Reviews. Clinical Oncology*. 2023; 20: 624–639.
- [2] Siegel RL, Miller KD, Fuchs HE, Jemal A. Cancer statistics, 2022. *CA: a Cancer Journal for Clinicians*. 2022; 72: 7–33.
- [3] Xia C, Dong X, Li H, Cao M, Sun D, He S, *et al.* Cancer statistics in China and United States, 2022: profiles, trends, and determinants. *Chinese Medical Journal*. 2022; 135: 584–590.
- [4] Wang H, Xu T, Huang Q, Jin W, Chen J. Immunotherapy for Malignant Glioma: Current Status and Future Directions. *Trends in Pharmacological Sciences*. 2020; 41: 123–138.
- [5] Kosti P, Opzomer JW, Larios-Martinez KI, Henley-Smith R, Scudamore CL, Okesola M, *et al.* Hypoxia-sensing CAR T cells provide safety and efficacy in treating solid tumors. *Cell Reports. Medicine*. 2021; 2: 100227.
- [6] Long GV, Menzies AM, Scolyer RA. Neoadjuvant Checkpoint Immunotherapy and Melanoma: The Time Is Now. *Journal of Clinical Oncology: Official Journal of the American Society of Clinical Oncology*. 2023; 41: 3236–3248.
- [7] Reck M, Remon J, Hellmann MD. First-Line Immunotherapy for Non-Small-Cell Lung Cancer. *Journal of Clinical Oncology: Official Journal of the American Society of Clinical Oncology*. 2022; 40: 586–597.
- [8] Wei J, Liu Y, Wang C, Zhang Y, Tong C, Dai G, *et al.* The model of cytokine release syndrome in CAR T-cell treatment for B-cell non-Hodgkin lymphoma. *Signal Transduction and Targeted Therapy*. 2020; 5: 134.
- [9] Monk BJ, Enomoto T, Kast WM, McCormack M, Tan DSP, Wu X, *et al.* Integration of immunotherapy into treatment of cervical cancer: Recent data and ongoing trials. *Cancer Treatment Reviews*. 2022; 106: 102385.
- [10] Agarwal S, Afaq F, Bajpai P, Behring M, Kim HG, Varambally A, *et al.* BZW2 Inhibition Reduces Colorectal Cancer Growth and Metastasis. *Molecular Cancer Research: MCR*. 2023; 21: 698–712.
- [11] Hiraishi H, Oatman J, Haller SL, Blunk L, McGivern B, Morris J, *et al.* Essential role of eIF5-mimic protein in animal development is linked to control of ATF4 expression. *Nucleic Acids Research*. 2014; 42: 10321–10330.
- [12] Wu CH, Sahoo D, Arvanitis C, Bradon N, Dill DL, Felsner DW. Combined analysis of murine and human microarrays and ChIP analysis reveals genes associated with the ability of MYC to maintain tumorigenesis. *PLoS Genetics*. 2008; 4: e1000090.
- [13] Jin X, Liao M, Zhang L, Yang M, Zhao J. Role of the novel gene BZW2 in the development of hepatocellular carcinoma. *Journal of Cellular Physiology*. 2019; 234: 16592–16600.
- [14] Li G, Lu A, Chen A, Geng S, Xu Y, Chen X, *et al.* BZW2/5MP1 acts as a promising target in hepatocellular carcinoma. *Journal of Cancer*. 2021; 12: 5125–5135.
- [15] Ge J, Mu S, Xiao E, Tian G, Tao L, Li D. Expression, oncological and immunological characterizations of BZW1/2 in pancreatic adenocarcinoma. *Frontiers in Genetics*. 2022; 13: 1002673.
- [16] Beroukhi R, Mermel CH, Porter D, Wei G, Raychaudhuri S, Donovan J, *et al.* The landscape of somatic copy-number alteration across human cancers. *Nature*. 2010; 463: 899–905.
- [17] Monaco G, Lee B, Xu W, Mustafah S, Hwang YY, Carré C, *et al.* RNA-Seq Signatures Normalized by mRNA Abundance Allow Absolute Deconvolution of Human Immune Cell Types. *Cell Reports*. 2019; 26: 1627–1640.e7.
- [18] Thorsson V, Gibbs DL, Brown SD, Wolf D, Bortone DS, Ou Yang TH, *et al.* The Immune Landscape of Cancer. *Immunity*. 2019; 51: 411–412.
- [19] Bonneville R, Krook MA, Kautto EA, Miya J, Wing MR, Chen HZ, *et al.* Landscape of Microsatellite Instability Across 39 Cancer Types. *JCO Precision Oncology*. 2017; 2017: PO.17.00073.
- [20] Malta TM, Sokolov A, Gentles AJ, Burzykowski T, Poisson L, Weinstein JN, *et al.* Machine Learning Identifies Stemness Features Associated with Oncogenic Dedifferentiation. *Cell*. 2018; 173: 338–354.e15.
- [21] Zeng D, Li M, Zhou R, Zhang J, Sun H, Shi M, *et al.* Tumor Microenvironment Characterization in Gastric Cancer Identifies Prognostic and Immunotherapeutically Relevant Gene Signatures. *Cancer Immunology Research*. 2019; 7: 737–750.
- [22] Yoshihara K, Shahmoradgoli M, Martínez E, Vegesna R, Kim H, Torres-García W, *et al.* Inferring tumour purity and stromal and immune cell admixture from expression data. *Nature Communications*. 2013; 4: 2612.
- [23] Jin Y, Wang Z, He D, Zhu Y, Chen X, Cao K. Identification of novel subtypes based on ssGSEA in immune-related prognostic signature for tongue squamous cell carcinoma. *Cancer Medicine*. 2021; 10: 8693–8707.
- [24] Aran D, Hu Z, Butte AJ. xCell: digitally portraying the tissue

- cellular heterogeneity landscape. *Genome Biology*. 2017; 18: 220.
- [25] Maeser D, Gruener RF, Huang RS. oncoPredict: an R package for predicting in vivo or cancer patient drug response and biomarkers from cell line screening data. *Briefings in Bioinformatics*. 2021; 22: bbab260.
- [26] Yang W, Soares J, Greninger P, Edelman EJ, Lightfoot H, Forbes S, *et al*. Genomics of Drug Sensitivity in Cancer (GDSC): a resource for therapeutic biomarker discovery in cancer cells. *Nucleic Acids Research*. 2013; 41: D955–D961.
- [27] Charoentong P, Finotello F, Angelova M, Mayer C, Efremova M, Rieder D, *et al*. Pan-cancer Immunogenomic Analyses Reveal Genotype-Immunophenotype Relationships and Predictors of Response to Checkpoint Blockade. *Cell Reports*. 2017; 18: 248–262.
- [28] Wang YQ, Wu DH, Wei D, Shen JY, Huang ZW, Liang XY, *et al*. TEAD4 is a master regulator of high-risk nasopharyngeal carcinoma. *Science Advances*. 2023; 9: eadd0960.
- [29] Cheng DD, Li SJ, Zhu B, Yuan T, Yang QC, Fan CY. Downregulation of BZW2 inhibits osteosarcoma cell growth by inactivating the Akt/mTOR signaling pathway. *Oncology Reports*. 2017; 38: 2116–2122.
- [30] Sato K, Masuda T, Hu Q, Tobo T, Gillaspie S, Niida A, *et al*. Novel oncogene 5MP1 reprograms c-Myc translation initiation to drive malignant phenotypes in colorectal cancer. *EBioMedicine*. 2019; 44: 387–402.
- [31] Huang L, Chen S, Fan H, Ai F, Sheng W. BZW2 promotes the malignant progression of colorectal cancer via activating the ERK/MAPK pathway. *Journal of Cellular Physiology*. 2020; 235: 4834–4842.
- [32] Wang S, Bai W, Huang J, Lv F, Bai H. Prognostic significance of BZW2 expression in lung adenocarcinoma patients. *International Journal of Clinical and Experimental Pathology*. 2019; 12: 4289–4296.
- [33] Kozel C, Thompson B, Hustak S, Moore C, Nakashima A, Singh CR, *et al*. Overexpression of eIF5 or its protein mimic 5MP perturbs eIF2 function and induces ATF4 translation through delayed re-initiation. *Nucleic Acids Research*. 2016; 44: 8704–8713.
- [34] Huang X, Yang Z, Li Y, Long X. m6A methyltransferase METTL3 facilitates multiple myeloma cell growth through the m6A modification of BZW2. *Annals of Hematology*. 2023; 102: 1801–1810.
- [35] Pös O, Radvanszky J, Buglyó G, Pös Z, Rusnakova D, Nagy B, *et al*. DNA copy number variation: Main characteristics, evolutionary significance, and pathological aspects. *Biomedical Journal*. 2021; 44: 548–559.
- [36] Voskarides K, Giannopoulou N. The Role of *TP53* in Adaptation and Evolution. *Cells*. 2023; 12: 512.
- [37] Fan J, To KKW, Chen ZS, Fu L. ABC transporters affects tumor immune microenvironment to regulate cancer immunotherapy and multidrug resistance. *Drug Resistance Updates: Reviews and Commentaries in Antimicrobial and Anticancer Chemotherapy*. 2023; 66: 100905.
- [38] Hegde S, Leader AM, Merad M. MDSC: Markers, development, states, and unaddressed complexity. *Immunity*. 2021; 54: 875–884.
- [39] Wang YH, Lin CC, Yao CY, Hsu CL, Hou HA, Tsai CH, *et al*. A 4-gene leukemic stem cell score can independently predict the prognosis of myelodysplastic syndrome patients. *Blood Advances*. 2020; 4: 644–654.